An improved method of energy calibration for position-sensitive silicon detectors*

Ming-Dao Sun(孙明道)[1,2,3] Tian-Heng Huang(黄天衡)[1] Zhong Liu(刘忠)[1;1)] Bing Ding(丁兵)[1]
Hua-Bin Yang(杨华彬)[1,2,3] Zhi-Yuan Zhang(张志远)[1] Jian-Guo Wang(王建国)[1] Long Ma(马龙)[1,2,3]
Lin Yu(郁琳)[1,2] Yong-Sheng Wang(王永生)[1] Zai-Guo Gan(甘再国)[1] Xiao-Hong Zhou(周小红)[1]

[1] Institute of Modern Physics, Chinese Academy of Sciences, Lanzhou 730000, China
[2] University of Chinese Academy of Sciences, Beijing 100049, China
[3] School of Nuclear Science and Technology, Lanzhou University, Lanzhou 730000, China

Abstract: Energy calibration of resistive charge division-based position-sensitive silicon detectors is achieved by parabolic fitting in the traditional method, where the systematic variations of vertex and curvature of the parabola with energy must be considered. In this paper we extend the traditional method in order to correct the fitting function, simplify the procedure of calibration and improve the experimental data quality. Instead of a parabolic function as used in the traditional method, a new function describing the relation of position and energy is introduced. The energy resolution of the 8.088 MeV α decay of ^{213}Rn is determined to be about 87 keV (FWHM), which is better than the result of the traditional method, 104 keV (FWHM). The improved method can be applied to the energy calibration of resistive charge division-based position-sensitive silicon detectors with various performances.

Keywords: resistive charge division, position-energy correlation, energy calibration, energy resolution

PACS: 29.40.Gx, 29.30.Ep, 25.70.Hi **DOI:** 10.1088/1674-1137/40/4/046202

1 Introduction

Fusion-evaporation is an important reaction channel in the synthesis of heavy nuclei. Evaporation residues are separated from beam particles as well as transfer products by an electromagnetic separation device [1], and implanted into a position-sensitive silicon detector (PSSD). New isotopes are usually identified by establishing α decay chains leading to known transitions; PSSDs allow position and time correlations between implanted nuclei and subsequent α decays to be achieved. The PSSD used in the present work is an X1-300 manufactured by the Micron Corporation (UK). This detector is ion-implanted with an active area of 50 mm×50 mm and a thickness of 300 μm. The silicon detector is fully depleted when a reverse bias of about 30 V is applied. One surface of the detector, which has a well-distributed resistive layer, is divided into 16 strips, with each strip 3 mm wide. Signals are output from the two ends of each strip. The other side of the detector is evaporated with a thin layer of aluminum and used to get the total signal of the silicon. In the present work, three PSSDs are installed side by side to form an implantation detector array.

The calibration of detectors is essential for data analysis. In the traditional method [2, 3], the correction of linear calibration is performed by a parabolic function, where the systematic variations of vertex and curvature of the parabola with energy must be considered, which makes the procedure of calibration complex. For the purposes of correcting the fitting function, simplifying the procedure of calibration and improving the quality of experimental data obtained in the ^{20}Ne+^{209}Bi reaction, an improved method of energy calibration of PSSD is presented.

In the following two sections, the improved method of energy calibration of PSSD will be introduced, and then the calibration results of this method and the traditional method [2, 3] will be compared through some long-lived α emitters produced in the ^{20}Ne+^{209}Bi reaction.

2 Energy and position calibration of PSSD

Signals output from the two ends of each strip are amplified in a preamplifier and main amplifier before being input into an ADC (Analog to Digital Converter),

Received 23 June 2015
* Supported by '100 Person Project' of the Chinese Academy of Sciences and the National Natural Science Foundation of China (11405224 and 11435014)
1) E-mail: liuzhong@impcas.ac.cn

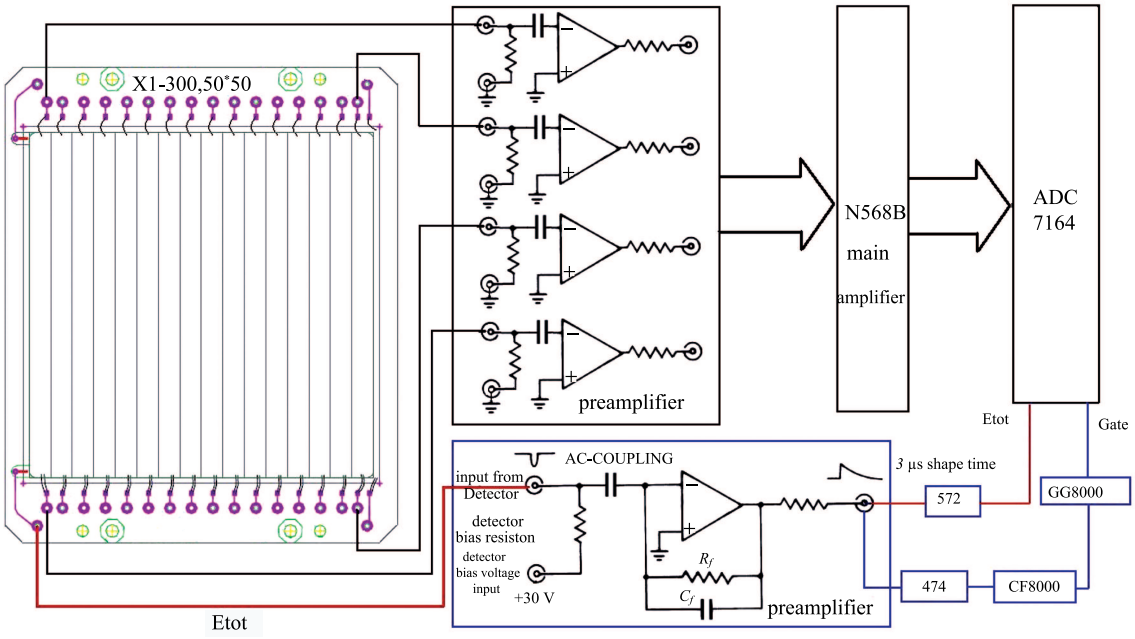

Fig. 1. (color online) A schematic diagram of PSSD and electronics.

see Fig. 1.

The position of an event along the strip is determined by the resistive charge division [4], while the resolution of position depends on the performance of the detector and noise from the electronics. The energy registered in one strip is the sum of energy output from the two ends of the strip. The position perpendicular to the strip is given by the strip number.

In Fig. 2, the two-dimensional spectrum of signals from the two ends of a strip for external α sources is plotted. The sources are: ^{239}Pu (5.157 MeV), ^{241}Am (5.486 MeV) and ^{244}Cm (5.805 MeV) [5], which correspond to the three groups of events in the middle of Fig. 2.

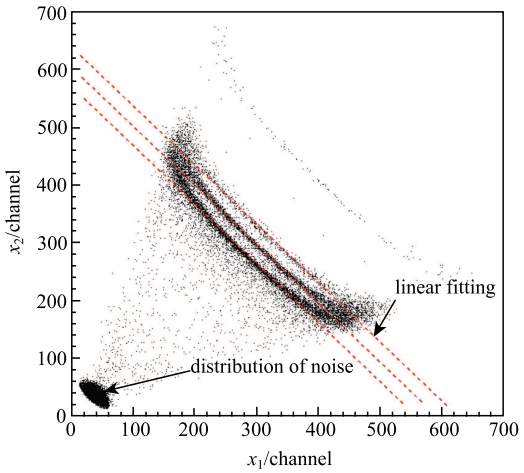

Fig. 2. (color online) A representative two dimensional spectrum of the raw energy signals from the two ends of one strip.

Three abnormal phenomena are observed in Fig. 2. First, each of the three groups of events is not linearly distributed, but curved. Additionally, this non-linearity is much greater at the two ends of the strip than at its center. The same phenomenon was initially reported in reference [6]. Although non-linearity caused by the rise-time effect [7−9] has the same form, its magnitude obtained from the known time constants is smaller than the experimental results. The variation of the system gain, i.e., the ratio between pulse height (channel) and energy (MeV), with position along the strip leads to this distortion [6]. Secondly, the deviation caused by noise is position dependent. Three types of noise are presented for a similar detector in reference [10], i.e., the noise from the input transistor of the amplifier, thermal noise from the resistive layer and shot noise produced by the leakage current of the detector, which is mainly caused by radiation damage. The amplifier noise and shot noise are larger at the ends of the strip than at its center [10]. Because the detector tested here is old enough and the radiation damage is rather serious, shot noise is assumed to be the main reason leading to this distortion. Lastly, the data points are limited to a finite sector region in Fig. 2, and do not extend to the coordinate axes. This results from the finite input impedance of the preamplifier and can be restored by a simple relation [11], based on the consideration that the detector is in series with the two preamplifiers. This situation can be improved by an appropriate design of preamplifier and an increase of the integral time of the main amplifier. However, the increasing of integral time may result in the enlarging of the electronic noise [9].

Due to the first distortion mentioned above, a linear calibration of energy is not enough. An improved method, which could be applied more universally to silicon detectors based on the resistive charge division, is presented below.

2.1 Linear calibration of energy

The energies E_1 and E_2 extracted from the two ends of a strip are proportional to their ADC amplitudes x_1 and x_2, respectively,

$$E_1 = a_1 x_1 + b_1, \tag{1}$$

$$E_2 = a_2 x_2 + b_2. \tag{2}$$

The total energy E is

$$E = E_1 + E_2. \tag{3}$$

Then, a relation of E and x_1, $x_2$can be obtained:

$$x_2 = -\frac{a_1}{a_2}x_1 + \frac{1}{a_2}E - \frac{b_1+b_2}{a_2}. \tag{4}$$

Three parameters $k_0 = -\dfrac{a_1}{a_2}$, $\dfrac{1}{a_2}$ and $b_{\rm sum} = \dfrac{b_1+b_2}{a_2}$ can be obtained by linear fitting of data points (Fig. 2), where b_1 and b_2 are parameters to be determined later. Then, the energy obtained by linear calibration can be written as

$$E = a_2(-k_0 x_1 + x_2 + b_{\rm sum}). \tag{5}$$

It is supposed that the center of noise distribution (shown in the lower corner of Fig. 2), namely the maximum of noise distribution density, is situated at the middle of a strip [2]. This assumption is confirmed by a test in Ref. [10]. So the output energies E_1 and E_2 corresponding to this center are equal. From Eqs. (1) and (2), we have

$$a_1 x_{n1} + b_1 = a_2 x_{n2} + b_2, \tag{6}$$

where x_{n1} and x_{n2} are the ADC amplitudes of noise at this center, and b_1 and b_2 can be obtained from $b_{\rm sum}$ and Eq. (6).

2.2 Position calibration

As in Ref. [3], the position along a strip can be determined by the difference between energies E_1 and E_2 extracted from the two ends of the strip. The relative position η is given as

$$\eta = \frac{E_1 - E_2}{E_1 + E_2}, \tag{7}$$

where E_1 and E_2 are the results of linear calibration of energy, shown in Eqs. (1) and (2). Relative position η gives the position relative to the geometrical center of a strip, the range of which is between -1 and 1. Introducing Eqs. (1) and (2) into Eq. (7), we have

$$\eta = \frac{a_1 x_1 - a_2 x_2 + (b_1 - b_2)}{a_1 x_1 + a_2 x_2 + (b_1 + b_2)}. \tag{8}$$

The relation between real position P and relative position is

$$P = \frac{L}{2} \times \eta, \tag{9}$$

where L is the length of the strip, L=50 mm here.

2.3 Improvement of energy calibration

The energy resolution can be improved by position-energy correlation based on the result of linear calibration.

The abnormal phenomena presented above can still be observed in Fig. 3, where the relation of relative position η and energy E obtained from linear calibration is described. The events close to the ends of each strip (see Fig. 3) cannot be distinguished for different α sources, therefore only the events around the central part, encircled with colored lines (see Fig. 3), are chosen in the improvement of linear calibration. When an event occurs at one end of a strip, the output at the other end will ideally be zero, and the range of η will be the interval from -1 to 1. However, as mentioned above, due to the existence of input impedance of the preamplifier, the range of relative position obtained by the resistive charge division is narrowed. It can be seen in Fig. 3 that the relative position η spans approximately between -0.5 and 0.5.

From Eqs. (3) and (7), we have

$$\frac{E}{E_1} = \frac{2}{1+\eta}, \tag{10}$$

defining

$$g = \frac{2}{1+\eta}, \tag{11}$$

then

$$\frac{E}{E_1} = g. \tag{12}$$

Eq. (12) indicates a linear relation between E/E_1 and g, but the data deviate from this simple relation. In Fig. 4, the selected events of the three α lines in Fig. 3 are plotted in the g-E/E_1 coordinate system. These three groups of events nearly overlap and follow a smooth curve. As a result, a new function, $f(g)$, is introduced

$$\frac{E}{E_1} = f(g) \tag{13}$$

to describe the actual relation between E/E_1 and g.

Different functions have been tried fitting the data points in Fig. 4, and a function with the following simple form

$$f(g) = Ag^2 + Bg + Cg^{1/2} + D \tag{14}$$

is found to be among the best. The results of linear calibration are improved by this function and new results are shown in Fig. 5 for all the data in Fig. 3.

There is some energy loss in the dead layer for the external α sources due to the existence of the dead layer of the detector. So for the internal α sources, the energy calibrated by the external α sources is larger than their real values. In order to remove this difference, some long-lived residues in the ^{20}Ne+^{209}Bi reaction are used to make a linear correction for the result obtained above. We have

$$E=[E_1(Ag^2+Bg+Cg^{1/2}+D)]K+M, \qquad (15)$$

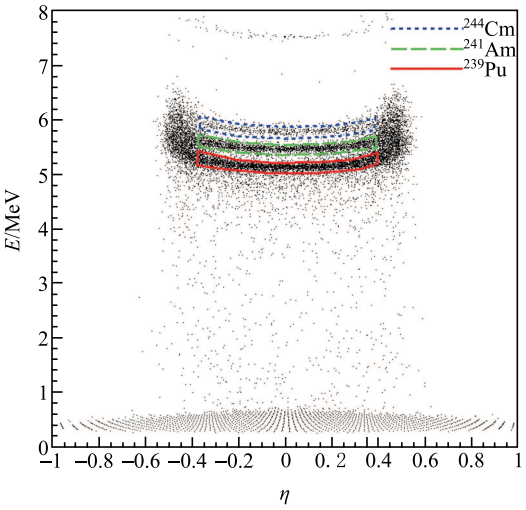

Fig. 3. (color online) Two dimensional spectrum of relative position η and E, the energy obtained from linear calibration. Three groups of events circled by lines of different colors define good events of the three external α sources, which can be distinguished from each other.

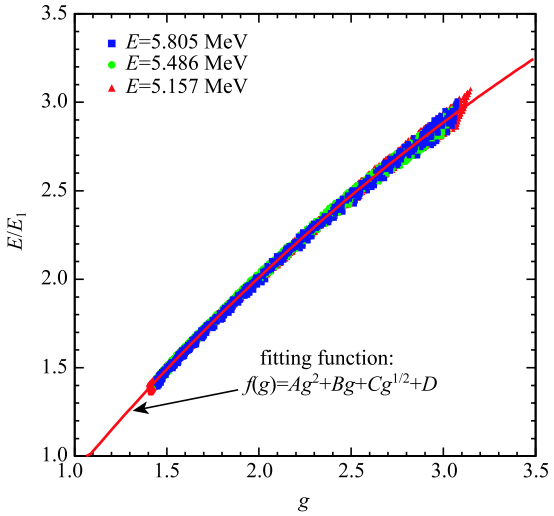

Fig. 4. (color online) Two dimensional spectrum of g and E/E_1 for the selected events in Fig. 3, see text for explanation.

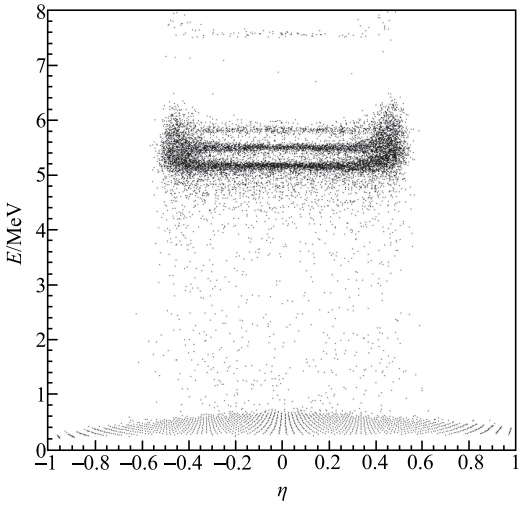

Fig. 5. (color online) Two dimensional spectrum of relative position η and E, the energy obtained from improved method.

where $K$and M are the parameters of this linear correction.

3 Comparison of calibration results obtained by the improved method and traditional method

This improved method has been applied in the experimental study of the ^{20}Ne+^{209}Bi reaction performed on the gas filled separator SHANS in Lanzhou [12]. The beam energies were 111.4 MeV and 122.6 MeV for ^{20}Ne.

The calibrated results by the improved method and traditional method for the α decays of some isotopes produced in the ^{20}Ne+^{209}Bi reaction are presented in

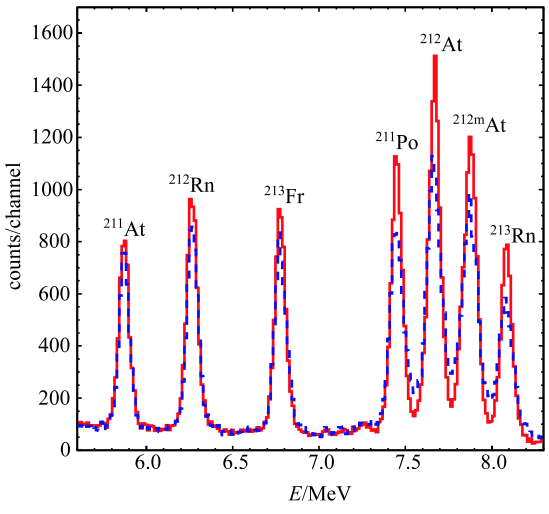

Fig. 6. (color online) A comparison between calibrated results by improved method (red line) and traditional method (dashed blue line).

Fig. 6, while the energy resolutions obtained are listed in Table 1. It is obvious that the improved method produces better results than the traditional one, especially for the α decays with higher energies.

Table 1. Comparison of energy resolutions.

nuclei	α decay energy/MeV	energy resolution (FMHW)/keV	
		improved	traditional
^{211}At	5.870	77	79
^{212}Rn	6.264	78	80
^{213}Fr	6.775	80	85
^{211}Po	7.450	83	94
^{212}At	7.679	88	98
^{212m}At	7.837	99	114
^{213}Rn	8.088	87	104

For the α decay (8.088 MeV) of the transfer reaction residue ^{213}Rn in the ^{20}Ne+^{209}Bi reaction, the energy resolution is determined to be 87 keV (FWHM), which is better than the result of the traditional method, 104 keV. The position resolution is determined to be less than 2 mm (FWHM), similar to the result of the traditional method. The position resolution is determined from the differences between the positions of short-lived implanted nuclei and those of the subsequent α decays. The resolution of position is not improved comparing with the result of traditional method, which may result from the significant noise (see Fig. 2). Noise reduction can improve the resolution of both energy and position.

4 Summary

An improved method of energy calibration for a position-sensitive silicon detector is introduced based on the observation that the distributions of data in the g-E/E_1 coordinate system are almost identical for different α sources (see Fig. 4). Compared with the traditional method, the procedure is simpler and the obtained energy resolutions are better. Different functions can easily be tried in the improved method, therefore detectors with non-linear performances (see Fig. 2) can be calibrated by this improved method, especially detectors for which the characteristic (namely the two-dimensional spectrum of position and energy) does not have a parabolic shape.

The authors are indebted to Professor TAN Ji-Lian for his useful discussions.

References

1 C. E. Düllmann, Nucl. Instrum. Methods Phys. Res. B, **266**: 4123-4130(2008)
2 C. M. Folden, Development of odd Z projectile reactions for transactinide element synthesisy, Ph.D. Thesis (USA: University of California, 2004)
3 G. B. JIA, Z. Y. ZHANG, M. H. HUANG et al, Nuclear Electronics & Detection Technology, **31**(7): 783-788(2011) (in Chinese)
4 J. L. Alberi, V.Radeka, IEEE Trans. Nuc. Sci, **23**(1): 251-258(1976)
5 E. Browne, J. K. Tuli, Nucl. Data Sheets, **122**: 205-293(2014); M. S. Basunia, Nucl. Data Sheets, **107**: 2323-2422(2006); B. Singh, E. Browne, Nucl. Data Sheets, **109**: 2439-2499(2008)
6 S. B. Kaufman, B. D. Wilkins, M. J. Fluss et al, Nucl. Instrum. Methods, **82**: 117-121(1970)
7 S. Kalbitzer, W. Melzer, Nucl. Instrum. Methods, **56**: 301-304(1967)
8 A. Doehring, S. Kalbitzer, W. Melzer, Nucl. Instrum. Methods, **59**: 40-44(1968)
9 W. Melzer, F. Pühlhofer, Nucl.Instrum.Methods, **60**: 201-204(1968)
10 D. Bassignana, E. Currasb, M. Fernandez et al, Nucl. Instrum. Methods Phys. Res. A, **732**: 186-189(2013)
11 Z. Z. LI, H. S. PENG, W. M. XIAO et al, Nuclear Electronics & Detection Technology, **4**: 200-203(1984) (in Chinese)
12 Z. Y. ZHANG, Experimental Study of the Superheavy Nuclide ^{271}Ds on the Gas-Filled Recoil Separator in Lanzhou, Ph. D. Thesis (Lanzhou: Institute of Modern Physics, CAS, 2012)(in Chinese)